All-Manganite Tunnel Junctions with Interface-Induced Barrier Magnetism

By *Z. Sefrioui, C. Visani, M. J. Calderón, K. March, C. Carrétéro, M. Walls, A. Rivera-Calzada, C. León, R. Lopez Anton, T. R. Charlton, F. A. Cuellar, E. Iborra, F. Ott, D. Imhoff, L. Brey, M. Bibes,* J. Santamaria,* and *A. Barthélémy*

The recent discovery of unexpected phases at oxide interfaces provides new insights into the physics of strongly correlated electron systems. The possibility of tailoring the electronic structure of such interfaces has triggered a great technological drive to functionalize them into devices. Here, we report the creation of an insulating phase with a significant interface-induced magnetic moment and its use as an active barrier in magnetic tunnel junctions. This phase appears at the interface between two manganese perovskite oxides, one being ferromagnetic-metallic (FM-M) and the other antiferromagnetic-insulating (AFM-I), and mimics a spin-filter behavior. Our results show that uncompensated moments at engineered magnetic interfaces may be a promising route to generate spin-polarized currents, circumventing the issues of spin-filter (SF) materials scarcity and offering new opportunities for antiferromagnets – by far the most numerous high temperature magnetic materials – in spintronics.

[*] Dr. M. Bibes
Unité Mixte de Physique CNRS/Thales associée à l'Université Paris-Sud
Campus de Polytechnique
1 Avenue A. Fresnel 91767 Palaiseau (France)
E-mail: manuel.bibes@thalesgroup.com
Dr. C. Carrétéro, Prof. A. Barthélémy
Unité Mixte de Physique CNRS/Thales associée à l'Université Paris-Sud
Campus de Polytechnique
1 Avenue A. Fresnel 91767 Palaiseau (France)
Dr. Z. Sefrioui, Dr. C. Visani, Dr. A. Rivera-Calzada, Prof. C. León, Dr. F. A. Cuellar, Prof. J. Santamaria
Grupo de Física de Materiales Complejos
Universidad Complutense de Madrid
28040 Madrid (Spain)
Dr. M. J. Calderón, Prof. L. Brey
Instituto de Ciencia de Materiales de Madrid, CSIC
Cantoblanco, 28049 Madrid (Spain)
Dr. K. March, Dr. M. Walls
Laboratoire de Physique des Solides, CNRS
Université Paris-Sud
91405 Orsay (France)
Dr. R. L. Anton, Dr. T. R. Charlton, Dr. D. Imhoff
ISIS, Rutherford Appleton Laboratory
Chilton, Oxon OX11 0QX (United Kingdom)
Dr. E. Iborra
Universidad Politécnica de Madrid
Escuela Técnica Superior de Ingenieros de Telecomunicaciones
28040 Madrid (Spain)
Dr. F. Ott
Laboratoire Léon Brillouin CEA/CNRS
UMR 12, 91191 Gif-sur-Yvette (France)

DOI: 10.1002/adma.201002067

The wealth of physical phenomena exhibited by materials with strong electronic correlations constitutes an exciting playground for solid-state scientists and a world of opportunities for novel devices.[1,2] Their range of functionalities spans from superconductivity to ferromagnetism in the bulk and can be further broadened by considering their interfaces.[3] Indeed, the symmetry breaking at the interface and the ensuing electronic or atomic reconstruction may result in unexpected properties. Examples are the conducting state at the interface between two insulators[4,5] which may be magnetic[6] or superconducting,[7] the interface ferromagnetism induced between two paramagnets,[8] or the suppressed magnetism near manganite-cuprate interfaces.[9]

Substantial theoretical work[3,10,11,12] has highlighted the role played by a number of interface phenomena (modified screening, band bending, polarity mismatch) in the determination of electronic parameters (bandwidth, on-site Coulomb interaction) potentially responsible for profound changes in the local charge, spin and orbital structure. In this regard, the possibility of artificially manipulating spin states at interfaces is particularly attractive in the framework of spintronics. Mixed-valence manganites are ideal systems for the investigation of this issue due to their intrinsic tendency to change their electronic properties in response to small perturbations.[2,13] Recent studies suggested that the magnetic state of ultrathin AFM manganite layers can be modified at the interface with a half-metallic $La_{2/3}Sr_{1/3}MnO_3$ layer.[10,14,15] As interfaces are key to the operation of spintronics systems (such as magnetic tunnel junctions MTJs), engineered interfaces with a different ground state may enhance the response of current devices and inspire novel spin-based architectures with additional functionalities.

To explore this route we have combined $La_{0.7}Ca_{0.3}MnO_3$ (LC3MO), a highly spin-polarized FM-M with a Curie temperature (T_C) of 270 K,[16] with $La_{0.3}Ca_{0.7}MnO_3$ (LC7MO), a charge-ordered insulator below 260 K, becoming AFM below 150 K.[17] As we show in the following, the good lattice matching and chemical compatibility between these materials allows the growth of heterostructures with high quality interfaces.[18] The physical properties of LC3MO/LC7MO interfaces were determined from complementary measurements on three types of samples: (1) [LC3MO/LC7MO] superlattices and (2) LC3MO/

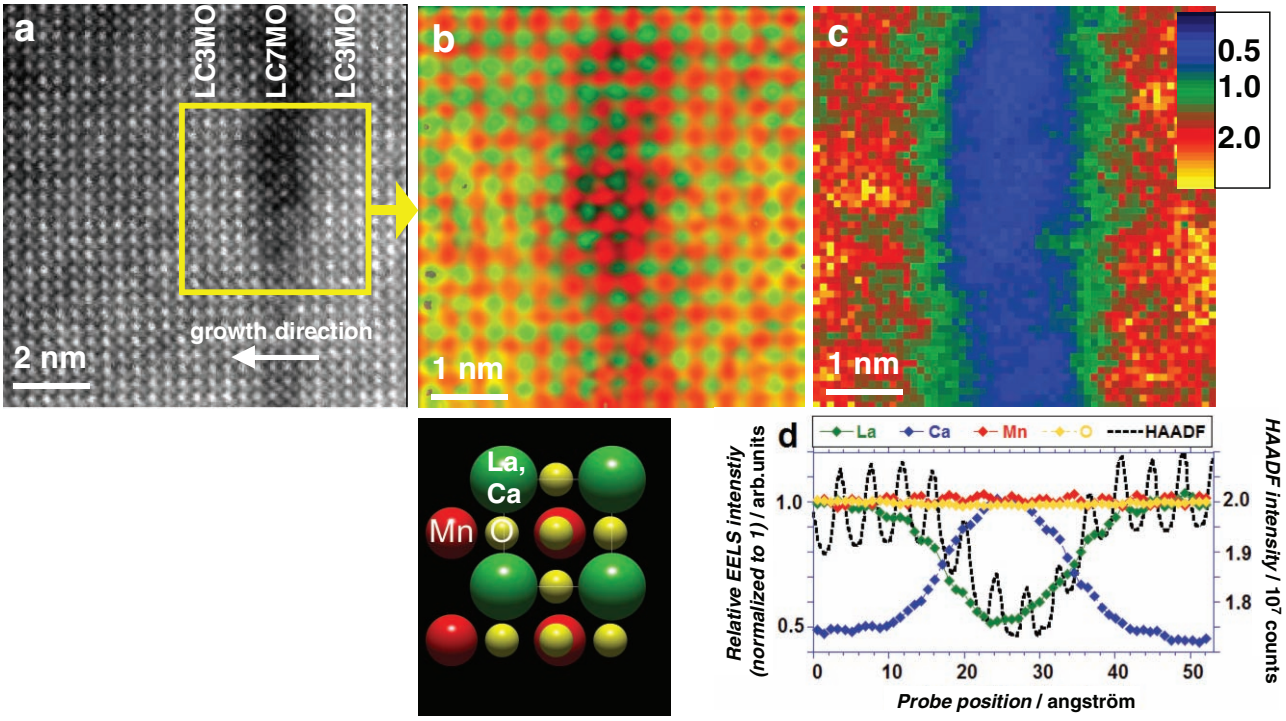

Figure 1. Atomic-scale structural and chemical characterization. (a) Raw HAADF UltraSTEM image of a LC3MO/LC7MO/LC3MO interface area. (b) Chemical map of atomic columns obtained from the combination of the La (green) and Mn (red) maps. The corresponding projected structure of LCMO is represented below. (c) Mapping of the La/Ca concentration ratio collected from the same spectrum image. (d) Average EELS intensity profiles corresponding to La, Ca, Mn, and O core-loss signals. The HAADF profile is superimposed.

LC7MO/LC3MO trilayers grown on $SrTiO_3$(001) (STO) and (3) LC3MO/LC7MO bilayers grown on Nb-STO(001). In all samples, the thickness of the LC7MO layers was 3 unit cells (~1.2 nm).

The structural, chemical and electronic properties of our heterostructures were characterized using a scanning transmission electron microscope (UltraSTEM, see Supporting Information) on a LC3MO(10 nm)/LC7MO(1.2 nm)/LC3MO(13 nm)// STO(001) sample. The high-angle annular dark-field (HAADF) image (**Figure 1a**) reveals, with an atomic resolution, the presence of the barrier layer richer in the light element Ca (darker contrast). Electron energy loss spectroscopy (EELS) combined with the spectrum-image technique allows the extraction of the chemical map for La (green) and Mn (red) (Figure 1b). Figure 1c shows a mapping of the La/Ca ratio collected with a probe step of 0.9 Å. The elemental profiles of Ca, O, Mn and La, extracted using the spectrum-image technique and coupled to the HAADF profile are represented in Figure 1d. As expected from the nominal composition of the layers, the La/Ca atomic concentration ratio decreases from ~2 in the electrodes to ~0.5 in the insulating barrier. The elemental maps also suggest the stabilization of a one-unit-cell-thick interfacial layer with La/Ca ratio equal to 1. The Mn level remains perfectly stable throughout the structure, whereas a very slight decrease in oxygen (2%) is visible in the barrier. From the analysis of different regions, we infer that at either interface the chemical roughness is rarely more than one atomic step.

First insights on the magnetic structure of the LC3MO/LC7MO interfaces were gained from polarized neutron reflectivity (PNR) experiments (see supporting information). The PNR results are shown in **Figure 2a** and b. At 150 K (Figure 2a), both curves generated from the two polarized intensities, *R+* and *R–*, show two Bragg peaks resulting from the superlattice modulation. The first one is situated around 0.07 $Å^{-1}$, while the second one at around 0.14 $Å^{-1}$ is barely visible. Results from the fit to the data (inset) show an asymmetric profile in the LC3MO where the magnetization is enhanced close to the upper face of the AFM layer and reduced at the bottom side. A ~0.9 nm magnetically dead layer appears at the interface with the substrate. At this temperature, the magnetization in the LC7MO layers is close to zero.

At 5 K (Figure 2b), results from the fit (inset) show again an asymmetric profile in the LC3MO layers and a reduced magnetization at the interface with the substrate. Remarkably, a magnetic moment of about 200 emu/cm^3 (~1.3 μ_B/Mn) appears inside the LC7MO layers. Thus, the PNR results point to the appearance of a FM moment in the originally AFM-I barrier. Within the phase diagram of $La_{1-x}Ca_xMnO_3$ a FM insulating phase is only observed at low Ca content ($x \approx 0.10$),[2] i.e. far from the composition of the layers in our samples. However, at manganite interfaces and surfaces, electronic phases different from those of the bulk compounds may be stabilized.[11,14,19,20] In our case, a possible scenario would be that the FM-M electrodes alter the magnetic state of the ultrathin LC7MO layer, which acquires a finite FM moment, while remaining insulating.

We have theoretically checked this scenario by performing self-consistent calculations using a model[12,15,20,21] that includes the kinetic energy (double-exchange), the Jahn-Teller phonons,

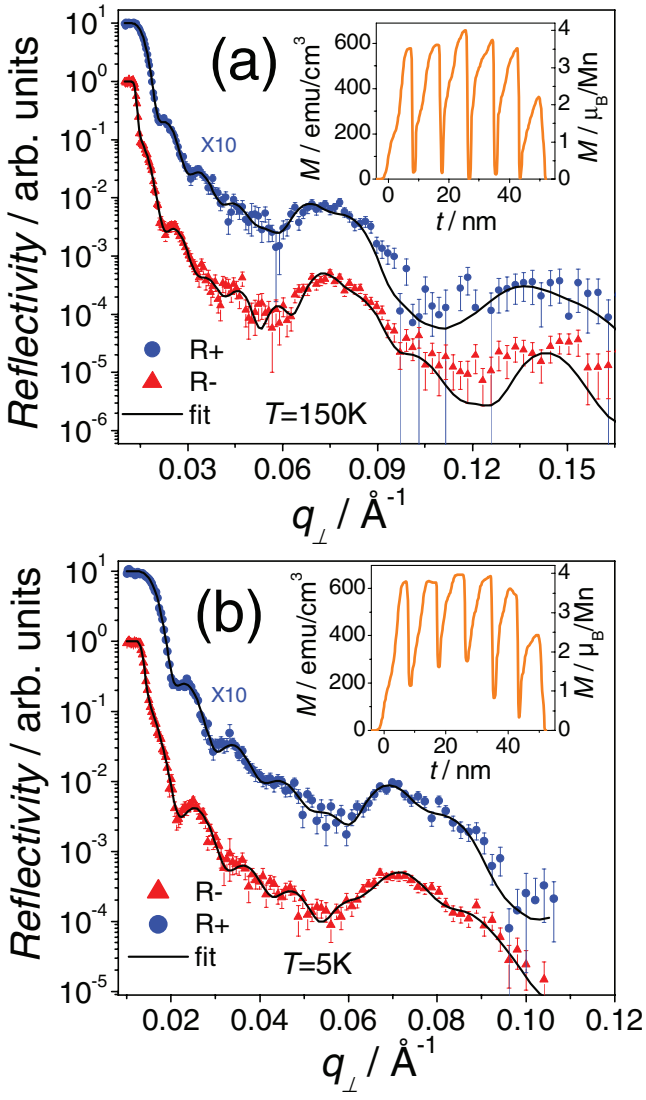

Figure 2. PNR data for a [LC3MO(7.5 nm)/LC7MO(1.2 nm)]$_5$/LC3MO (7.5 nm) superlattice at 150 K (a) and 5 K (b). The insets show the magnetic profiles deduced from the fits to the data.

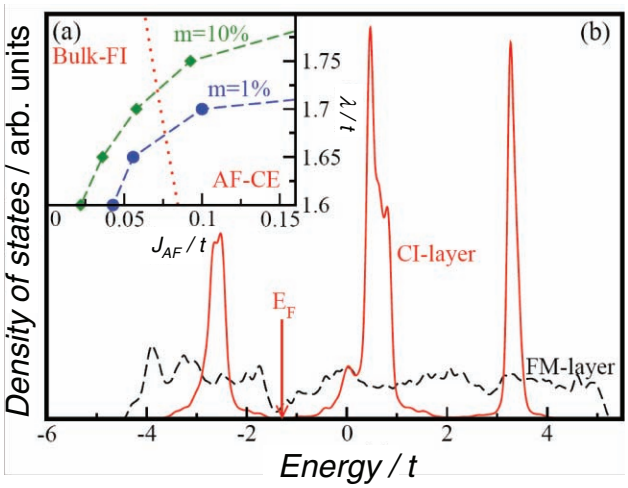

Figure 3. (a) Bulk phase diagram (dotted line) superimposed to that of the new canted states appearing in the multilayer (dashed lines with symbols) as a function of λ (Jahn-Teller coupling) and J_{AF} (AFM superexchange coupling). All quantities are in units of the hopping parameter $t \sim 0.2$ eV. For $\lambda > 1.6$ t, the bulk phase diagram consists of two phases: FM insulating (FI) for smaller J_{AF} and CE-type AFM for larger J_{AF}. In contrast, for the heterostructure, canted states, which do not appear in bulk, are favoured within the CE region (right of the dotted line). Circles correspond to a 1% magnetization, and diamonds to a 10% magnetization in the ultrathin LC5MO layer. (b) electronic density of states (DO) at the LC3MO FM layer (black-dashed line) and at the LC5MO canted insulating (CI) layer (solid-red line). The arrow indicates the position of the Fermi energy. DOS at the LC5MO barrier for the opposite spin orientation is shifted by $m_z J_H$, where J_H the Hund coupling of a Mn atom. The value of the m_z is about 10% of the bulk magnetization and results from spin canting in the CE phase (J_H is 2.5–3 eV, so the shift is 250–300 meV).

the AFM super-exchange, and the Coulomb interaction. The calculations were performed for LC3MO/$La_{0.5}Ca_{0.5}MnO_3$/LC3MO heterostructures. $La_{1-x}Ca_xMnO_3$ at $x = 0.5$ (LC5MO) shows a similar kind of CE-type AFM ordering as LC7MO[21] and has a smaller unit cell, simplifying the calculations. Furthermore, as shown by EELS, in the heterostructure the electronic density goes from 0.7 in the LC3MO layers to nearly 0.3 in the ultrathin LC7MO layer and we expect that the existence of a wide gap insulating phase for LC5MO may lead to pinning of the electron density at 0.5 in the ultrathin layer.[20] We have found that a LC5MO monolayer between two LC3MO FM electrodes acquires a finite FM moment and is insulating within a parameter range that would correspond to CE order in the bulk. The results are summarized in **Figure 3**. Figure 3b shows the density of states projected on the LC3MO FM-M layers and on the LC5MO layer with a canted AFM order (that corresponds to a 10% magnetization): at the Fermi energy E_F the LC5MO layer shows a gap (it is insulating) while the FM electrodes are conducting. The ultrathin LC5MO layer gains kinetic energy in the perpendicular direction by getting some FM moment while the Jahn-Teller coupling and the AFM super-exchange keep the FM moment rather small (though still consistent with the magnetization profiles (inset of Figure 3a) and the insulating behaviour). These results are reproduced over a wide range of parameters (Figure 3a). Our results for a CE-type manganite interface are consistent with the recent prediction of a FM tendency at the surface of these compounds.[19] Although the model calculation provides a theoretical footing for the existence of a FM insulating state in terms of canting of the CE phase, from the experimental results we cannot conclude on its detailed microscopic nature.

Equipped with this information, we then turned to investigate the impact of interface-induced magnetism of LC3MO/LC7MO interfaces on the tunneling properties of MTJs integrating a 1.2 nm LC7MO layer as the barrier and two LC3MO electrodes (see supporting information). **Figure 4a** shows tunnel magnetoresistance (*TMR*) curves measured with a bias voltage V = 10 mV at temperatures ranging from 6 K to 150 K. The *TMR* was defined as $TMR = (R_{AP} - R_P)/R_P = (I_P - I_{AP})/I_{AP}$ where P and AP subscripts refer to the antiparallel (AP) and parallel (P) magnetization configurations. It is clear from Figure 4a that the junction resistance switches sharply from

ADVANCED MATERIALS
www.advmat.de

www.MaterialsViews.com

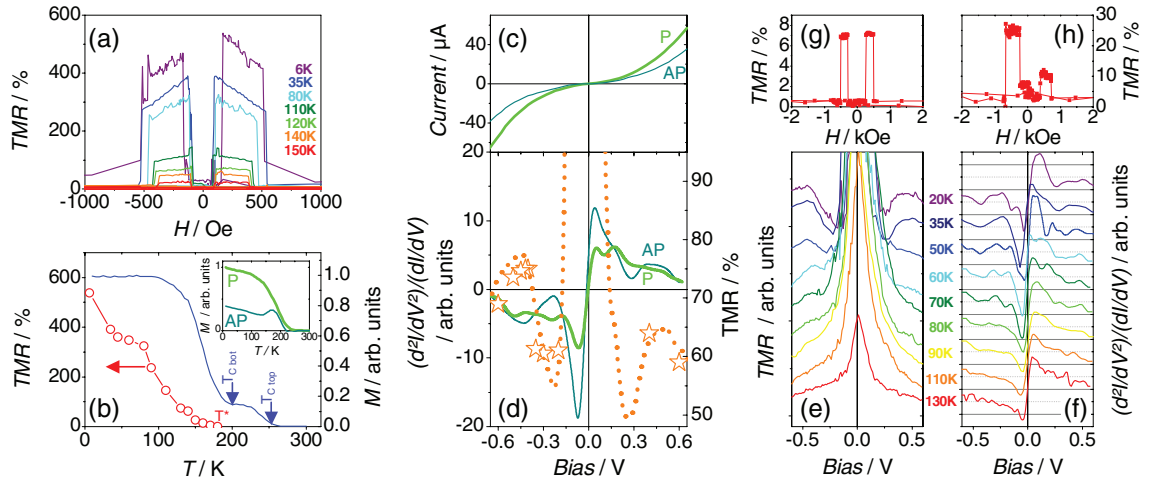

Figure 4. (a) *TMR* curves of a LC3MO(8 nm)/LC7MO(1.2 nm)/LC3MO(50 nm) MTJ at 10 mV and different temperatures. (b) Temperature dependence of the *TMR* (left axis) and of the difference between the magnetization (right axis) measured at 10 Oe (P state) and –60 Oe (AP state) (see inset) for a LC3MO(10 nm)/LC7MO(1.2 nm)/LC3MO(65 nm) sample. This plot emphasizes the signal from the LC3MO(10 nm) layer. (c) *I(V)* curves in the P and AP state at 35 K for a LC3MO(8 nm)/LC7MO(1.2 nm)/LC3MO(50 nm) junction. (d) TMR(V) curve deduced from the *I(V)* curves of (c) (dashed line) and from the R(H) curves measured at fixed voltage (symbols) (left axis) and bias dependence of $(d^2I/dV^2)/(dI/dV)$ derived from the data in (c). Thermal evolution of the *TMR* vs *V* (e) and $(d^2I/dV^2)/(dI/dV)$ vs *V* (f). (g) and (h) TMR versus magnetic field for two LC3MO (20 nm) / LC7MO (1.2 nm) / Nb-STO tunnel junctions measured at $V = 10$ mV and 60 K.

the P to the AP state (and vice versa) due to the well-separated coercivities of the electrodes. At low temperature, a very large *TMR* of more than 500% is obtained. This is in striking contrast with previous results on junctions with AFM barriers and different manganite compositions such as [$La_{0.7}Ca_{0.3}MnO_3/La_{0.45}Ca_{0.55}MnO_3/La_{0.7}Ca_{0.3}MnO_3$][22] or [$La_{0.7}Sr_{0.3}MnO_3/La_{0.35}Ca_{0.65}MnO_3/La_{0.7}Sr_{0.3}MnO_3$],[23] for which *TMR* values lower than ~20% have been reported. The low *TMR* values may result from spin depolarization at the FM/AFM interface as discussed in references.[22,23] It is also important to note that the *TMR* vanishes at $T^* \approx 180$ K, close to the Curie temperature of the bottom LC3MO electrode ($T_C \approx 190$ K) (Figure 4b and inset). This indicates that the magnetism of the FM electrodes is only marginally depressed at the electrode-barrier interfaces. While in high-quality MTJs based on $La_{2/3}Sr_{1/3}MnO_3$ the difference between T^* and T_C can be rather small,[24,25] it is usually larger with LC3MO electrodes,[16] possibly due to the reduced robustness of the double-exchange.[26,27] The high structural quality of our MTJs and the good compatibility between the electrode and barrier materials are certainly partly responsible for these excellent magnetotransport properties. The large *TMR* values suggest that the electrodes are highly spin-polarized, as expected from their predicted half-metallic nature.[28] As we show in the following, the response of these junctions is not only determined by the electrodes but also by novel interface-induced phases.

To fully characterize the spin-dependent transport mechanisms, we have measured the *I(V)* curves in the P and AP states (Figure 4c). The *I(V)* curves are non-linear, in agreement with a tunnel-type transport, and the current in the P state is always larger than in the AP state resulting in a positive *TMR*. The *TMR(V)* calculated from the *I(V)* curves (dashed line in Figure 4d) and the *R(H)* data (symbols in Figure 4d) agree well with each other and a virtually symmetric dependence is obtained, as expected for MTJs with similar electrodes. At low bias, the *TMR* decreases rapidly down to about ±200 mV, as occurs in conventional manganite-based MTJs,[29] possibly due to magnon excitations.[30] Upon further increasing the bias voltage, the *TMR* exhibits a significant increase up to ±450 mV and finally gradually decreases again for larger bias values. This non-monotonic dependence differs fundamentally from that found in conventional MTJs (*TMR* progressively decreases over the whole bias range.[29,31]) In fact, the increase in the *TMR* with bias observed between ~200 and ~450 mV recalls the behavior of MTJs with FM tunnel barriers, also called *spin-filters* (SF).[32–35]

In SF, electrons tunneling through a thin FM insulator in which the conduction band is spin-split by exchange experience different barrier heights depending on their spin ($\Phi_\uparrow$ for spin-up and $\Phi_\downarrow$ for spin-down). Because the tunneling probability *T(E)* is an exponential function of the barrier height this results in a highly spin-polarized current. The *TMR* of SF is expected to increase with bias,[36] first smoothly, and then more abruptly when the energy of the tunneling electrons exceeds the lower barrier height. Indeed, just above this energy $e\Phi_\uparrow$, transport still occurs by direct tunneling (DT) for minority-spin electrons while majority-spins electrons traveling by Fowler-Nordheim tunneling (FNT) carry a larger current. Upon further raising the bias voltage the *TMR* attains a maximum when the energy of the tunneling electrons exceeds the barrier height for minority spins ($\Phi_\downarrow$) and finally decreases gradually.[36] This expected behavior of the *TMR(V)* in SF has been found and analyzed in EuS-based junctions.[36] Beyond the low-bias anomaly, this is also what we observe in our junctions (see Figure 4d).

Further support to the spin-filtering picture can be obtained from plots of $(d^2I/dV^2)/(dI/dV) \sim d(\log T(E))/dV$ as a function of *V*[36,37] (see Figure 4d). The analysis of the $(d^2I/dV^2)/(dI/dV)$ data in the P or AP configuration allows for the detection of the transitions between the DT and FNT regimes for majority ($\Phi_\uparrow$)

and minority ($\Phi_\downarrow$) spins, respectively. In the low-bias range, both the *TMR* and $(d^2I/dV^2)/(dI/dV)$ show strong variations.[30] Beyond this regime, one can identify maxima at about ±200 mV and ±450 mV in the P and AP configuration, respectively, which, within the scenario of Nagahama et al.,[36] correspond to $\Phi_\uparrow$ and $\Phi_\downarrow$. We note that these values match well the voltages at which the *TMR* starts to increase and decrease, respectively, as expected. This strongly supports an interpretation of our transport data in terms of spin-filtering. As spin-filtering necessarily requires tunneling through a FM barrier, we infer from this analysis the existence of an insulating state with a substantial FM moment in our junctions. It is important to note that, while the giant *TMR* values observed at low applied bias may not be generated by spin filtering alone but also by the contribution of the highly spin polarized electrodes, the enhanced *TMR* found at high bias essentially results from spin filtering.

More information on this FM-insulating state can be extracted from the temperature dependence of the spin-dependent transport data. In Figure 4e and 4f we plot the thermal evolution of the bias dependence of the *TMR* and $(d^2I/dV^2)/(dI/dV)_{ap}$ respectively. Two characteristic signatures of SF, namely the maxima in *TMR(V)* and $(d^2I/dV^2)/(dI/dV)_{ap}$ progressively disappear as *T* increases, both vanishing at T_{SF} between 90 K and 110 K. This qualitative change of behavior with temperature is not observed in MTJs with non-magnetic barriers, in which the *TMR(V)* is mostly determined by the DOS of the electrode and the electronic structure of the barrier.[38] We argue that the change observed at T_{SF} signals the transition from a FM-like to a paramagnetic state and we thus estimate its Curie temperature as about 100 K.

To obtain a direct confirmation that spin-filtering occurs at the LC3MO/LC7MO interface, we also investigated junctions in which one of the FM electrodes was replaced by a non-magnetic metal. In this case, spin-filtering is the only mechanism that may produce a *TMR* effect: upon tunneling from the non-magnetic metal across the FM insulating state (with a spin-split DOS), the electrons whose spin direction corresponds to the lowest barrier height are preferentially transmitted into the FM electrode acting as a spin analyzer. The resistance is thus large (small) when the magnetizations of the two FM elements are AP (P). Junctions based on LC3MO(20 nm)/LC7MO(1.2 nm) bilayers deposited onto a 1%-Nb-doped STO single-crystalline substrate were patterned. On Figure 4g and 4h, we show two typical TMR curves obtained for different junctions at 60 K. The clear resistance switching with magnetic field provide a solid confirmation of spin filtering and definitely show that a FM insulating state is induced in the nominally AFM LC7MO layer.

In summary, we have demonstrated that a large ferromagnetic moment can be induced at interfaces in a nominally antiferromagnetic insulating oxide. This interface-induced magnetic state can be functionalized into a spin-filtering tunnel barrier operating in the high bias range and at temperatures comparable to or better than most other spin-filter materials (notably Eu chalcogenides[33] or $(La,Bi)MnO_3$[39,40]). Extending our approach to antiferromagnetic oxides with high ordering temperature should expand dramatically the range of simple spin-filter materials and inspire novel concepts in oxide spintronics.

Experimental Section

Films were grown on (001) $SrTiO_3$ substrates in a high-pressure (3.4 mbar) pure oxygen sputtering system at high temperatures (900 °C). Magnetic tunnel junctions have been defined by UV lithography (see Supporting Information). More details about the NION Ultra-STEM and EELS experiments can also be found in the Supporting Information section.

Supporting Information

Supporting Information is available from the Wiley Online Library or from the author.

Acknowledgements

We would like to thank J. Villegas, V. Garcia, V. Cros, R. Mattana, A. Anane and C. Colliex for fruitful discussions, N. Bonnet and J. Cutrona for the use of their PCA-AFC code and O. Krivanek, N. Dellby and the Nion Company staff for their assistance. Z. S. acknowledges financial support from Universidad Complutense de Madrid and M.J.C. from the Ramon y Cajal Program. This work was supported by the Spanish Ministry for Science and Education programs MAT 2005–06024, MAT2008 06517, FIS2009–08744 and CONSOLIDER INGENIO 2010 CSD2009–00013 (IMAGINE), CAM under PHAMA grant S2009/Mat-1756, and the Réseau Thématique de Recherche Avancée "Triangle de la Physique".

Received: June 4, 2010
Published online: September 7, 2010

[1] E. Dagotto, *Science* **2005**, *309*, 257.
[2] M. Imada, A. Fujimori, Y. Tokura, *Rev. Mod. Phys.* **1998**, *70*, 1039.
[3] S. Okamoto, A. J. Millis, *Nature* **2004**, *428*, 630.
[4] A. Ohtomo, H. Y. Hwang, *Nature* **2004**, *427*, 423.
[5] M. Basletic, J.-L. Maurice, C. Carrétéro, G. Herranz, O. Copie, M. Bibes, E. Jacquet, K. Bouzehouane, S. Fusil, A. Barthélémy, *Nature Mater.* **2008**, *7*, 621.
[6] A. Brinkman, M. Huijben, M. Van Zalk, J. Huijben, U. Zeitler, J. C. Maan, W. G. Van der Wiel, G. Rijnders, D. H. A. Blank, H. Hilgenkamp, *Nat. Mater.* **2007**, *6*, 493.
[7] N. Reyren, S. Thiel, A.D. Caviglia, L. Fitting Kourkoutis, G. Hammerl, C. Richter, C. W. Schneider, T. Kopp, A.-S. Rüetschi, D. Jaccard, M. Gabay, D. A. Muller, J.-M. Triscone, J.Mannhart, *Science,* **2007**, *317*, 1196.
[8] K. S. Takahashi, M. Kawasaki, Y. Tokura, *Appl. Phys. Lett.* **2001**, *79*, 1324.
[9] A. Hoffmann, S. G. E. te Velthuis, Z. Sefrioui, J. Santamaria, M. R. Fitzsimmons, S. Park, M. Varela, *Phys. Rev. B* **2005**, *72*, 140407(R).
[10] S. Yunoki, A. Moreo, E. Dagotto, S. Okamoto, S. S. Kancharla, A. Fujimori, *Phys. Rev. B* **2007**, *76*, 064532.
[11] B. R. K. Nanda, S. Satpathy, M. S. Springborg, *Phys. Rev. Lett.* **2007**, *98*, 216804.
[12] M. J. Calderón, J. Salafranca, L. Brey, *Phys. Rev. B* **2008**, *78*, 024415.
[13] K. H. Ahn, T. Lookman, A. R. Bishop, *Nature* **2004**, *428*, 401.
[14] D. Niebieskikwiat, M. B. Salamon, L. E. Hueso, N. D. Mathur, J. A. Borchers, *Phys. Rev. Lett.* **2007**, *99*, 247207.
[15] J. Salafranca, M. J. Calderón, L. Brey, *Phys. Rev. B* **2008**, *77*, 014441.
[16] M. H. Jo, N. D. Mathur, N. K. Todd, M. G. Blamire, *Phys. Rev. B.* **2000**, *61*, R14905.
[17] M. T. Fernandez-Diaz, J. L. Martinez, J. M. Alonso, E. Herrero, *Phys. Rev. B* **1999**, *59*, 1277.

[18] V. Peña, Z. Sefrioui, D. Arias, C. Leon, J. Santamaria, M. Varela, S. J. Pennycook, J. L. Martinez, *Phys Rev. B.* **2004**, *69*, 224502.
[19] S. Dong, R. Yu, S. Yunoki, J.-M. Liu, E. Dagotto, *Phys. Rev. B* **2008**, *78*, 064414.
[20] L. Brey, *Phys. Rev. B* **2007**, *75*, 104423.
[21] L. Brey, *Phys. Rev. Lett.* **2004**, *92*, 127202.
[22] M. H. Jo, M. G. Blamire, D. Ozkaya, A K. Petford-Long, *J. Phys: Condens. Matter* **2003**, *15*, 5243.
[23] L. M. B. Alldredge, Y. Suzuki, *Appl. Phys. Lett.* **2004**, *85*, 437.
[24] V. Garcia, M. Bibes, A. Barthélémy, M. Bowen, E. Jacquet, J.-P. Contour, A. Fert, *Phys. Rev. B.* **2004**, *69*, 052403.
[25] Y. Ishii, H. Yamada, H. Sato, H. Akoh, Y. Ogawa, M. Kawasaki, Y. Tokura, *Appl. Phys. Lett.* **2006**, *89*, 042509.
[26] A. A. Sidorenko, G. Allodi, R. De Renzi, G. Balestrino, M. Angeloni, *Phys. Rev. B* **2006**, *73*, 054406.
[27] M. Bibes, Ll. Balcells, S. Valencia, J. Fontcuberta, M. Wojcik, E. Jedryka, S. Nadolski, *Phys. Rev. Lett.* **2001**, *87*, 067210.
[28] W. E. Pickett, D. J. Singh, *Phys. Rev. B* **1996**, *53*, 1146.
[29] M. Bowen, A. Barthélémy, M. Bibes, E. Jacquet, J.-P. Contour, A. Fert, F. Ciccacci, L. Duo, R. Bertacco, *Phys. Rev. Lett.* **2005**, *95*, 137203.
[30] S. Zhang, P. M. Levy, A. C Marley, S. P. P. Parkin, *Phys. Rev. Lett.* **1997**, *79*, 3744.
[31] E. Y. Tsymbal, E. N. Mryasov, P. R. LeClair, *J. Phys.: Condens. Matter* **2003**, *15*, R109.
[32] L. Esaki, P. J. Stiles, S. von Molnar, *Phys. Rev. Lett.* **1967**, *19*, 852.
[33] J. S. Moodera, X. Hao, G. A. Gibson, R. Meservey, *Phys. Rev. Lett.* **1988**, *61*, 637.
[34] J. S. Moodera, T. S. Santos, T. Nagahama, *J. Phys.: Condens. Matter.* **2007**, *19*, 165202.
[35] A. V. Ramos, M.-J. Guittet, J.-.B. Moussy, R. Mattana, C. Deranlot, F. Petroff, C. Gatel, *Appl. Phys. Lett.* **2007**, *91*, 122107.
[36] T. Nagahama, T. S. Santos, J. S. Moodera, *Phys. Rev. Lett.* **2007**, *99*, 016602.
[37] S. Nishioka, R. Matsumoto, H. Tomita, T. Nozaki, Y. Suzuki, H. Itoh, S. Yuasa, *Appl. Phys. Lett.* **2008**, *93*, 122511.
[38] J. M. de Teresa, A. Barthélémy, A. Fert, J.-P. Contour, F. Montaigne, P. Seneor, *Science* **1999**, *286*, 507.
[39] M. Gajek, M. Bibes, A. Barthélémy, K. Bouzehouane, S. Fusil, M. Varela, J. Fontcuberta, A. Fert. *Phys. Rev. B* **2005**, *72*, 020406(R).
[40] M. Gajek, M. Bibes, S. Fusil, K. Bouzehouane, J. Fontcuberta, A. Barthélémy, A. Fert. *Nat. Mater.* **2007**, *6*, 296.